Appl. Sci. Converg. Technol. 24(6): 278-283 (2015)
http://dx.doi.org/10.5757/ASCT.2015.24.6.278

Research Paper

Electrical Bistable Characteristics of Organic Charge Transfer Complex for Memory Device Applications

Chang-Lyoul Lee*
Advanced Photonics Research Institute (APRI), Gwangju Institute of Science and Technology (GIST), 123 Cheomdan-gwagiro, Buk-gu, Gwangju 500-712, Korea

Received November 13, 2015; revised November 20, 2015; accepted November 23, 2015

Abstract In this work, the electrical bistability of an organic CT complex is demonstrated and the possible switching mechanism is proposed. 2,9-Dimethyl-4,7-diphenyl-1,10-phenanthroline (BCP) and tetracyanoquinodimethane (TCNQ) are used as an organic donor and acceptor, respectively, and poly-methamethylacrylate (PMMA) is used as a polymeric matrix for spin-coating. A device with the Al/(Al_2O_3)/PMMA:BCP:TCNQ[1:1:0.5 wt%]/Al configuration demonstrated bistable and switching characteristics similar to Ovshinsky switching with a low threshold voltage and a high ON/OFF ratio. An analysis of the current-voltage curves of the device suggested that electrical switching took place due to the charge transfer mechanism.

Keywords: Organic memory, Charge transfer complex, Electrical switching, Bistability, Retention, Filament

I. Introduction

During the last 30 years, tremendous progress has been made in electronics and opto-electronic devices based on organic and polymeric materials. These organic (polymer) electronics and opto-electronics devices have been realized by light-emitting diodes [1,2], thin-film transistors [3,4], solar cells [5,6], lasers [7] and other devices. Moreover, some of these devices, especially organic light-emitting diodes (OLED), have been commercialized. However, memory devices remain an exception given the rapid progress of opto-electronic devices, despite the fact that the switching phenomena in organic materials were originally reported more than 30 years ago [8-12].

Recently, considerable attention has been directed toward electrical switching and memory devices which consist of organic materials, polymers and charge transfer complexes with an electrical bistable function [13-31]. Memory devices based on organic (polymer) materials have many advantages compared to inorganic memory devices, such as flexibility, simple processing, a low cost, and large-area fabrication via printing technology. Moreover, it is possible to realize ultra-high-density memory through the stacking of several memory layers.

Several critical conditions must be satisfied before organic (polymer) memory devices can be used in practical applications. These conditions include a lower threshold voltage (<5 V), a higher ON/OFF ratio (>orders of 103), a rapid switching time (<100 ns), longer retention (>10 years at 60°C), higher duration (>106 cycles) and a high memory capacity (>109 bite). Among the several types of organic (polymer) memory devices, such as trapping filling [13], filamentary conduction [14,15], electrochromicity [16], electroreduction and conformation changes of molecules [17,18], organic/metal/organic (O/M/O) structures [19-22] and charge transfer (CT) complex [23-31], last two organic (polymer) memory devices, organic/metal/organic (O/M/O) structures and charge transfer (CT) complex, are entitled to be used for practical application. Especially, organic (polymer) memory devices based on the CT complex are expected to show fastest switching times (<10 ns), as the switching takes place *via* a rapid electronic process (redox reaction) rather than a slow process (chemical reaction, a conformational change, or isomerization), as reported in other memory devices.

An organic memory device based on the CT complex was initially reported by Potember et al., where the transition from the high-resistance state to the low-resistance state is realized by the charge transfer between copper and tetracyanoquinodimethane (TCNQ) [23]. However, due to the inhomogeneous film morphology and poor reversibility between the ON and OFF states, the device showed relatively poor reproducibility. In addition, switching from the ON to the OFF state can be only realized by the application of a short pulse of current or heat or by storing the device for extended periods of time without an external field.

Non-volatile organic memory devices based on the CT complex, which satisfy the critical requirements for

*Corresponding author
E-mail: vsepr@gist.ac.kr

practical applications, were first realized by the Prof. Adachi group [28]. T. Oyamada et al. demonstrated the switching effect of the Cu:TCNQ CT complex in the device structure of ITO/Al/(Al_2O_3)/Cu:TCNQ/Al. Writing and erasing were realized by applying positive and negative bias, respectively. The ON/OFF ratio was 104. The thin Al2O3 layer on an Al electrode, which has a large dielectrical constant, is responsible for the re-writable switching mechanism. The high built-in field which forms between the Al/Al2O3 and the CT complex layer controls the charge transfer between the donor and the acceptor.

After the Cu:TCNQ CT complex memory device was reported, several types of CT complex organic memory devices were reported by changing the copper metal donor with a different metal [24] or with an alkali-metal donor [25], or using new types of organic donors and acceptors [26,27] with different electron donating and accepting capabilities. In memory devices based on the CT complex, ON and OFF switching were realized by the formation and de-formation of the CT complex via an electron transfer between the donor and the acceptor [29-31]. Researchers also showed a fast switching time (<100 ns) and excellent device performance.

In the present work, the electrical bistability of an organic CT complex is demonstrated and a possible switching mechanism is proposed. 2,9-Dimethyl-4,7-diphenyl-1,10-phenanthroline (BCP) and tetracyanoquinodimethane (TCNQ) are used as an organic donor and acceptor, respectively, and poly-methamethylacrylate (PMMA) is used as a polymeric matrix for spin-coating. The CT complex composition, [PMMA:BCP:TCNQ=X:Y:Z wt%], is varied from 1:1:0.5 wt% to 1:1:3 wt% by only changing the TCNQ content and not changing the PMMA and BCP contents. Cyclohexanone was used as a solvent for the spin-coating. The fabricated memory device had a simple diode structure of Al/(Al_2O_3)/CT complex/Al. Both the top and bottom Al electrode had a width of 0.5 mm, resulting in a memory device with an active area of 0.25 mm^2.

II. Experimental

The bottom Al electrode (0.5 mm width and 60 nm thickness) was deposited onto a cleaned glass substrate by thermal evaporation (<5×10^{-6} torr). A thin Al_2O_3 layer is formed during the transfer of the Al-coated substrate to a clean bench for the CT complex spin-casting. CT complex films were formed by the spin-coating of a cyclohexanone solution of PMMA:BCP:TCNQ. The PMMA and BCP contents were both fixed at 1 wt% to the solvent, and TCNQ content was changed from 0.5 to 3 wt%. The CT complex films were thermally annealed at 120°C for 1 hour under a vacuum condition. The thickness of the CT complex films was approximately 30 nm. Finally, the 60 nm-thick top Al electrode was deposited onto the CT complex film through a shadow mask. The fabricated device has the Al(60 nm)/(Al2O3)/PMMA:BCP:TCNQ CT complex(30 nm)/Al(60 nm) structure, an electrically symmetrical structure, even with an Al_2O_3 layer existing between the bottom electrode and the CT complex layer. The surface morphology of the CT film was investigated by optical microscopy and atomic force microscopy (AFM). The current-voltage (*I-V*) characteristics of the CT complex memory device were measured with a Hewlett Packard 4155B semiconductor parameter analyzer. A molecular simulation was carried out with the MM/PM3 potential to investigate the electron density of the organic donor. All measurements were performed at room temperature in air.

III. Results and Discussion

The chemical structures of the materials used in this work and the device configuration are shown in Figure 1(a). The molecular simulation was conducted by the MM/PM3 potential method to investigate the electron density of the organic donor material. The spare electrons in the N groups of the BCP (the electron density of N groups are –0.205220 and –0.205022, respectively), two electron-withdrawing dicyanomethylene groups and the quinonoid ring in TCNQ [32] make it possible to utilize BCP and TCNQ as the

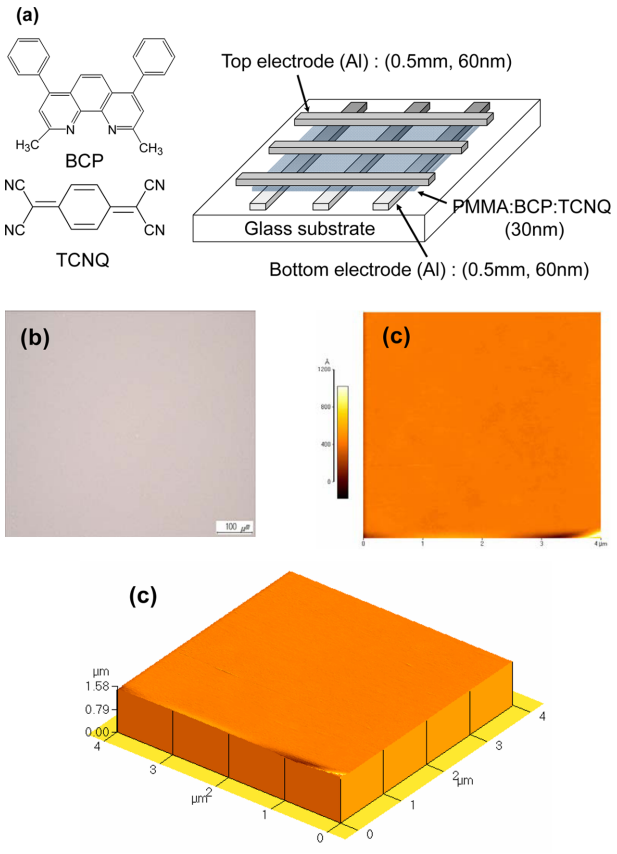

Figure 1. (a) Chemical structure of the materials and the device configuration used in this work. Optical microscopy (b) and AFM (c) images of the PMMA:BCP:TCNQ [1:1:1 wt%] CT complex film on a Si wafer.

electron donor and electron acceptor, respectively. The surface topographies of the PMMA:BCP:TCNQ film samples were investigated using an optical microscopy [Figure 1(b)] and an AFM [Figure 1(c)]. A very smooth surface morphology with height variation of less than ±2 nm, in contrast to the poly-crystalline properties of the Cu:TCNQ CT complex [23], was observed by AFM when the TCNQ content was less than 1 wt%, suggesting that the CT complex film was homogeneous with no phase separation or aggregation. However, when the TCNQ content exceeded 2 wt%, the phase separation of the TCNQ moiety was observed after 1 hour of annealing at 120°C in a vacuum. A uniform film morphology is a basic necessary condition to obtain high reproducibility as well as good device stability (operation lifetime). Therefore, a CT complex film containing less than 1 wt% of TCNQ was fabricated and used as an active layer for memory device applications.

Figure 2 shows the absorption spectra of pristine BCP, TCNQ, the BCP:TCNQ [1:1 mol] solution and the PMMA:BCP:TCNQ [1:1:0.5 wt% and 1:1:3 wt%] films. When the TCNQ (deep yellow color in acetonitrile and cyclohexanone) was added to the PMMA:BCP cyclohexanone solution, the color of the solution changed from whitish pale yellow to blackish dark blue. Given this color change, it is assumed that the CT complex was formed. As more direct evidence, the absorption spectrum of the PMMA:BCP:TCNQ [1:1:0.5 wt%] film confirmed the formation of the CT complex in the ground state. The characteristics of the CT band were observed in the region of 500-1000 nm, while there was no significant absorbance in the pristine BCP and TCNQ solutions. When the TCNQ content increased from 0.5 wt% to 3 wt% in the film, TCNQ neutral and radical absorption peaks were observed in the regions of 400 nm and 600-1000 nm [33], respectively, similar to that of the BCP:TCNQ [1:1 mol] solution, due to the strong electron affinity (2.8±0.1 eV) of the TCNQ acceptor [32]. These results confirm that maintaining a proper distance between the donor and acceptor by controlling the donor and acceptor content as well as using a polymer matrix are very important to generate the CT complex state.

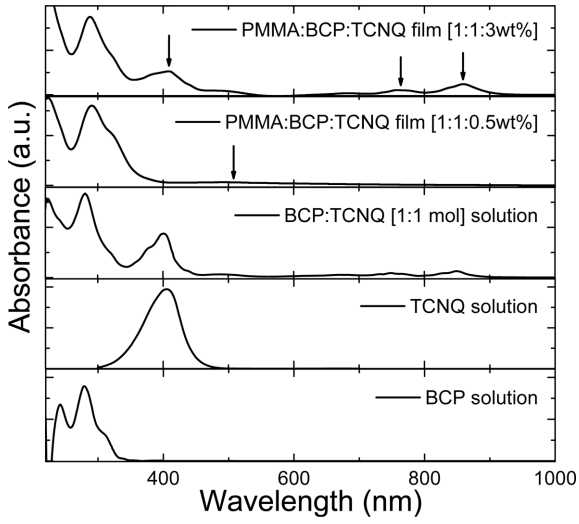

Figure 2. Absorbance spectra of the pristine BCP, TCNQ and BCP:TCNQ [1:1 mol] solutions and the PMMA:BCP:TCNQ [1:1:0.5 wt% and 1:1:3 wt%] films. Dichloromethane and acetonitrile were used as a solvent for the pristine BCP and TCNQ solutions, respectively. Cyclohexanone was used as solvent for the BCP:TCNQ [1:1 mol] solution and the PMMA:BCP:TCNQ [1:1:0.5 wt% and 1:1:3 wt%] films.

The current-voltage (*I-V*) characteristics of the PMMA :BCP:TCNQ [1:1:0.5 wt%] CT complex device are shown in Figure 3 (a). The device is initially in the high-resistance state (OFF state), remaining in the OFF state until the applied voltage is lower than the threshold voltage (V_{th}). When the applied voltage is higher than the threshold voltage (V_{th}), the transition from the high-resistance state (OFF state) to the low-resistance state (ON state) takes place (first bias scan). This process can be regarded as the "writing" process in memory devices. The different voltage scan direction (negative bias scan in the initial condition)

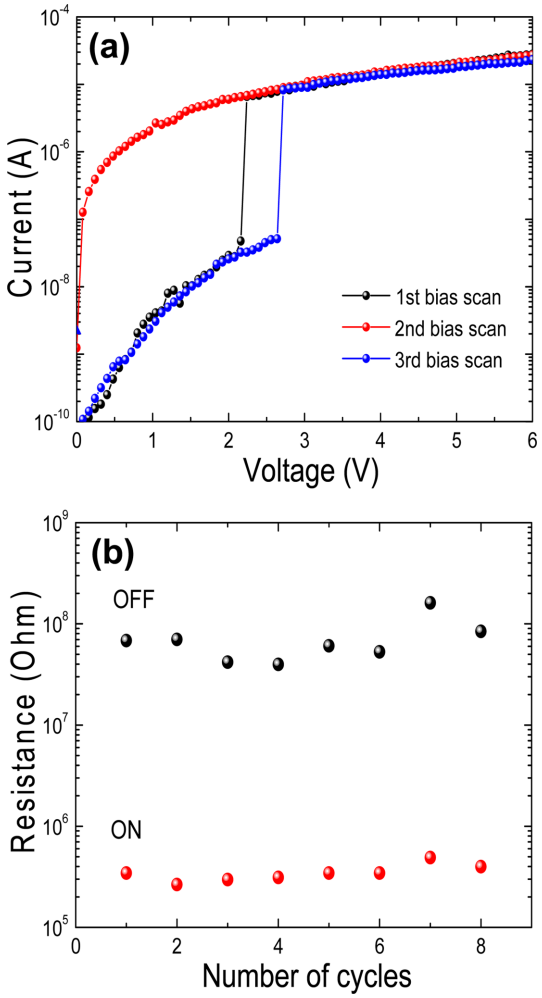

Figure 3. (a) Current-voltage (*I-V*) characteristics of the Al/(Al_2O_3)/PMMA:BCP:TCNQ [1:1:0.5 wt%]/Al CT complex device. (b) The resistance (conductivity) difference of the ON and OFF states with the number of bias scan cycles.

results in the same transition behavior due to the symmetrical device structure. After the device was in the ON state, a subsequent voltage scan (second bias scan) followed the ON state current. However, the device remained for some amount of time without any applied bias, the low-resistance state reverted to a high-resistance state (OFF state), changing to the ON state again by the third bias scan. These processes could be repeated several times, which can be considered as typical write-once-read-many (WORM) behavior. While there are some variations in the ON/OFF values, the conductivity (resistance) difference of the ON and OFF states is nearly three orders of magnitude, remaining quite stable with a number of bias scan cycles [Figure 3 (b)].

In order to study the retention time of the PMMA:BCP:TCNQ [1:1:0.5 wt%] CT complex in the ON state, different time delays of voltage scans were conducted after the device was in the ON state. The time delay was changed from 2 sec to 60 sec. As shown in Figure 4(a), when no bias scan was applied to the CT complex device within 20 sec, the ON state reverts back to the OFF state. This result indicates that the PMMA:BCP:TCNQ [1:1:0.5 wt%] CT complex device has a very short retention time in the ON state without applied voltage, thus showing promise as an Ovshinsky switcher [12,13].

Figure 4(b) shows the retention properties of the PMMA:BCP:TCNQ [1:1:0.5 wt%] CT complex device in the ON state at different applied voltages. The current of the device under a constant applied voltage was measured when the device was in the ON state. When the applied voltage (V) was lower than $V_{hold,}$ the ON state changed to the OFF state, but when the applied voltage was higher than V_{hold}, the ON state was maintained. These device properties, similar to a thyristor, make it possible to use this CT complex system as a voltage regulator for device protection and for volatile memory applications [13,34]. The device changes its resistance state from the OFF (0 state) to the ON state (1 state) when the applied voltage (V) is higher than V_{th} (writing process). When no bias is applied or when the applied voltage (V) to retain the ON

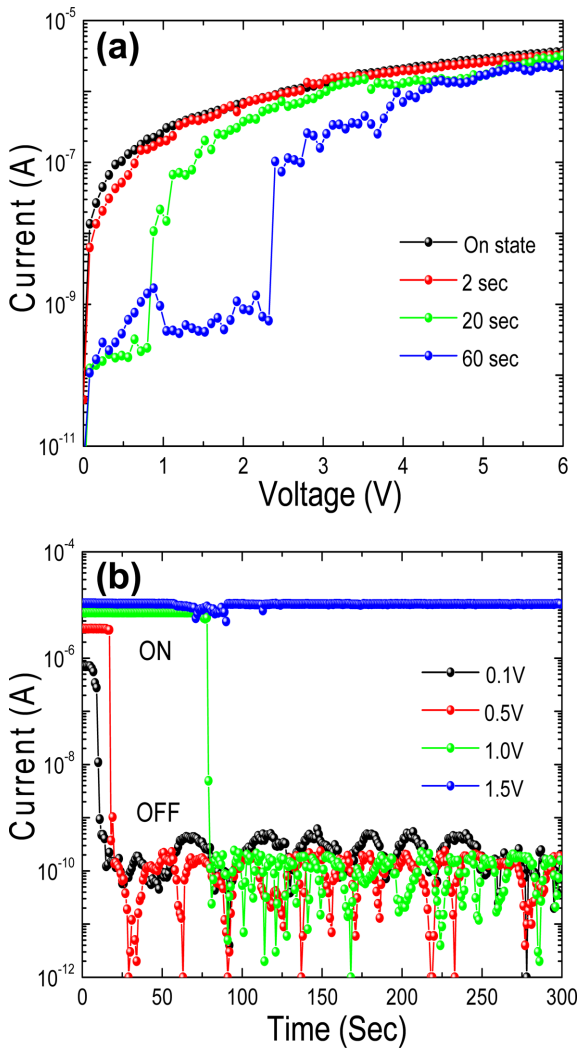

Figure 4. (a) Current-voltage (*I-V*) characteristics of the Al/(Al_2O_3)/PMMA:BCP:TCNQ [1:1:0.5 wt%]/Al CT complex device with a different time delay of the voltage scans after device is in the ON state. (b) Retention properties of the Al/(Al_2O_3)/PMMA:BCP:TCNQ [1:1:0.5 wt%]/Al CT complex device in the ON state at different applied voltages.

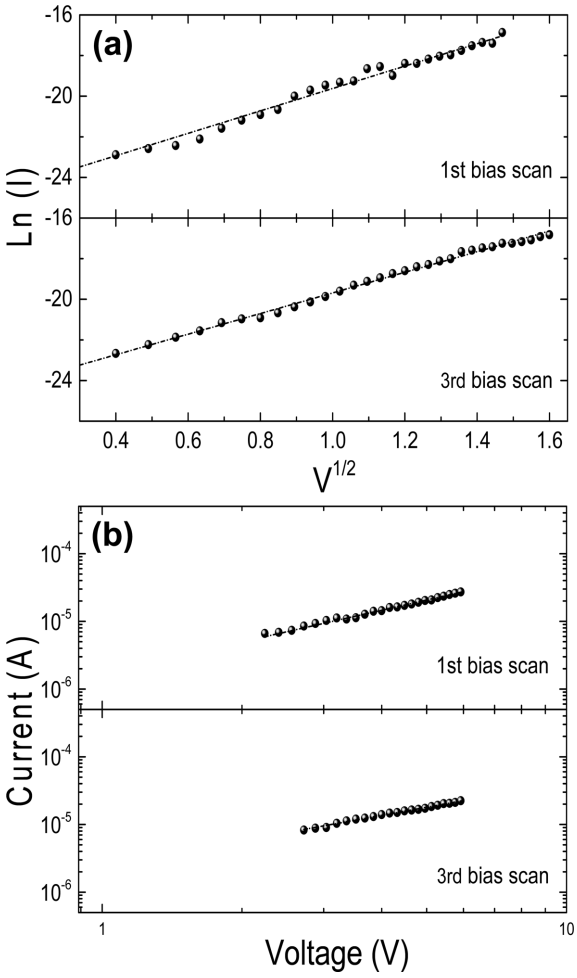

Figure 5. Results of the fitting of the current-voltage (*I-V*) curve of the Al/(Al_2O_3)/PMMA:BCP:TCNQ [1:1:0.5 wt%]/Al CT complex device in the ON (c) and OFF (d) states.

state is lower than V_{hold}, the ON state changed to OFF state and remained in the OFF state (erase process). A read process with the 0 or 1 state can be realized by applying voltage between Vhold<V<V_{th}. A somewhat lower or different current range in Figures 4(a) and (b) as compared to that in Figure 3(a) was observed. When the device properties were measured, the *I-V* curves were initially measured, with the other properties measured subsequently. Therefore, it is suspected that electrical breakdown and/or degradation of the device during its operation are among the reasons for these differences. Further experiments will be carried out to explain these device behaviors.

Among the several types of switching mechanisms, two switching (bistable) mechanisms, the charge transfer mechanism and filamentary conduction, are highly likely to explain the electrical switching phenomena of devices. An analysis of the current-voltage curves of the PMMA:BCP:TCNQ [1:1:0.5 wt%] CT complex device [Figure 5] suggested that the transition from the high-resistance to the low-resistance state took place due to the charge transfer mechanism [29-31]. The linear fitting of Ln(*I*) versus $V^{1/2}$ in the OFF state [Figure 5(a)] and of log I versus log V in the ON state [best fitting of log *I*-log *V* are $I \propto V^{1.56}$ during the first bias scan and $I \propto V^{1.24}$ in the third bias scan, Figure 5(b)] indicate that the current (charge transport) was controlled by the direct charge injection from Al to the CT complex (thermionic emission model [35,36]) in the OFF state and by the space-charge-limited current (SCLC) in the ON state [35, 37], and not by filament conduction, which results in metallic behavior [14,15] (log *I*-log V is $I \propto V^{1.0}$). Therefore, the switching (bistable) mechanism of the PMMA:BCP:TCNQ [1:1: 0.5 wt%] CT complex device is expected to be identical to that of the published metal-TCNQ CT complex device. In the OFF state, there is a complete charge transfer between the donor and acceptor such that *inter-site* coulomb repulsion between the electrons causes the organic materials initially to prohibit electrical transport. Above V_{th}, some neutral TCNQ molecules appear; these neutral TCNQ molecules provide a mixed valance state with existing TCNQ radical anion, and the mixed state TCNQ complex shows higher conductivity than those of the neutral TCNQ and CT complex with complete charge transfers.

However, several phenomena as described below leave strong doubt that the switching of the PMMA:BCP:TCNQ [1:1:0.5 wt%] CT complex device originated from filamentary conduction. The PMMA:BCP:TCNQ [1:1: 0.5 wt%] CT complex device showed very poor reproducibility (below 30%). Three or four pixels from nine pixels in the fabricated device showed bistable and switching performance. Changing the substrate also affected the reproducibility of the device. When the substrate was changed from glass to a particle-free SiO_2/Si wafer (thickness of SiO_2=3000A), fewer pixels in the fabricated device showed bistable and switching behaviors. Finally, the device did not show current or V_{th} dependence with a change of the active area in the pixel. These results strongly suggest that the conductivity change can be realized by the filament, as formed by defects or dust on the bottom of the substrate [15]. More experiments, such as the current and V_{th} variations according to the film thickness of the CT complex, the temperature, and the time-dependence of the conductivity of the device should be carried out to determine the switching mechanism of CT complex devices.

V. Conclusions

A volatile memory device based on the organic CT complex was demonstrated. The spare electrons in the N groups of BCP and the strong electron withdrawing properties of TCNQ cause the CT complex to enter the ground state, as confirmed by the color change and the absorbance spectra of the PMMA:BCP:TCNQ solution and the film. A device with the Al/(Al_2O_3)/PMMA:BCP:TCNQ[1:1:0.5 wt%]/Al configuration demonstrated bistable and switching characteristics similar to Ovshinsky switching with a low threshold voltage and a high ON/OFF ratio. An analysis of the current-voltage curves of the device suggested that electrical switching took place due to the charge transfer mechanism. However, several phenomena, such as poor reproducibility, no current and V_{th} dependence with variation of the active area in the pixel leave strong doubt that the switching of the PMMA:BCP:TCNQ CT complex device originated from filamentary conduction. Further investigations to reveal the switching mechanism are in progress.

Acknowledgments

This work was supported by the APRI Research Program through a grant provided by the Gwangju Institute of Science and Technology and by the Honam Sea Grant R&D Program of 2015.

References

[1] J. H. Burroughes, D. D. C. Bradley, A. R. Brown, R. N. Marks, K. Mackay, R. H. Friend, P. L. Burns, and A. B. Holmes, Nature 347, 539 (1990).
[2] T.-H. Han, Y. Lee, M.-R. Choi, S.-H. Woo, S.-H. Bae, B. H. Hong, J.-H. Ahn, and T.-W. Lee, Nat. Photonics 6, 105 (2012).
[3] H. Sirringhaus, N. Tessler, and R. H. Friend, Science 280, 1741 (1998).
[4] Y. Yuan, G. Giri, A. L. Ayzner, A. P. Zoombelt, S. C. B. Mannsfeld, J. Chen, D. Nordlund, M. F. Toney, J. Huang, and Z. Bao, Nat. Commun. 5, 3005 (2014).
[5] G. Yu, J. Gao, J. C. Hummelen, F. Wudl, and A. J. Heeger, Science 270, 1789 (1995).
[6] Y. Liu, J. Zhao, Z. Li, C. Mu, W. Ma, H. Hu, K. Jiang, H. Lin, H. Ade, and H. Yan, Nat. Mater. Nat. Commun. 5, 5293 (2014).
[7] N. Tessler, G. J. Denton, and R. H. Friend, Nature 382, 695 (1996).
[8] A. Szymanski1, D. C. Larson, and M. M. Labes, Appl. Phys. Lett. 14, 88 (1969).

[9] H. Carchano, R. Lacoste, and Y. Segui, Appl. Phys. Lett. 19, 414 (1971).
[10] H. K. Henisch and W. R. Smith, Appl. Phys. Lett. 24, 589 (1974).
[11] A. R. Elsharkawi and K. C. Kao, J. Phys. Chem. Solids. 38, 95. (1977).
[12] S. R. Ovshinsky, Phys. Rev. Lett. 21, 1450 (1968).
[13] D. Ma, M. Aguiar, J. A. Freire, and I. A. Hümmelgen, Adv. Mater. 12, 1063 (2000).
[14] D. Tondelier, K. Lmimouni, D. Vuillaume C. Fery, and G. Haas, Appl. Phys. Lett. 85, 5763 (2004).
[15] W. Tang, H. Shi, G. Xu, B. S. Ong, Z. D. Popovic, J. Deng, J. Zhao, and G. Rao, Adv. Mater. 17, 2307 (2005).
[16] T. Tsujoka and H. Kondo, Appl. Phys. Lett. 83, 937 (2003).
[17] A. Bandyopadhyay and A. J. Pal, Appl. Phys. Lett. 82, 1215 (2003).
[18] A. Bandyopadhyay and A. J. Pal, Appl. Phys. Lett. 84, 999 (2004).
[19] L. P. Ma, J. Liu, and Y. Yang, Appl. Phys. Lett. 80, 2997 (2002).
[20] L. P. Ma, S. M. Pyo, J. Ouyang, Q. F. Xu, and Y. Yang, Appl. Phys. Lett. 82, 1419 (2003).
[21] J. Wu, L. P. Ma, and Y. Yang, Phys. Rev. B 69, 115321 (2004).
[22] L. D. Bozano, B. W. Kean, V. R. Deline, J. R. Salem, and J. C. Scott, Appl. Phys. Lett. 84, 607 (2004).
[23] R. S. Potember, T. O. Poehler, and D. O. Cowon, Appl. Phys. Lett. 34, 405 (1979).
[24] Q. Zhang, W. Wang, G. Ye, X. Yan, Z. Zhnag, and Z. Hua, Synth. Met. 144, 285 (2004).
[25] X.-L. Mo, G.-R. Chen, Q.-J. Cai, Z.-Y. Fan, H.-H. Xu, Y. Ya, J. Yang, H.-H. Gu, and Z.-Y. Hua, Thin Solid Films 436, 259 (2003).
[26] J. Li, Z. Xue, W. M. Liu, S. Hou, X. Li, and X. Zhao, Phys. Lett. A 266, 441 (2000).
[27] K. Z. Wang, Z. Q. Xue, M. Ouyang, D. W. Wang, H. X. Zhang, and C. H. Huang, Chem. Phys. Lett. 243, 217 (1995).
[28] T. Oyamada, H. Tanaka, K. Matsushige, H. Sasabe, and C. Adachi, Appl. Phys. Lett. 83, 1252 (2003).
[29] J. Y. Ouyang, C.W. Chu, C. R. Szmanda, L. P. Ma and, Y. Yang, Nat. Mater. 3, 918 (2004).
[30] C. W. Chu, J. Y. Ouyang, J.-H. Tseug, and Y. Yang, Adv. Mater. 17, 1440 (2005).
[31] R. J. Tseng, J. Huang, J. Ouyang, R. B. Kaner, and Y. Yang, Nano Lett. 5, 1077 (2005).
[32] B. Milián, R. Pou-Amérigo, R. Viruela and E. Ortí, Chem. Phys. Lett. 391, 148 (2004).
[33] M. S. Matos and M. H. Gehlen, Spectroc. Acta Pt. A-Molec. Biomolec. Spectr. 60, 1421 (2004).
[34] R. M. Q. Mello, E. C. Azevedo, A. Meneguzzi, M. Aguiar, L. Akcelrud, and I. A. Hümmelgen, Macromol. Mater. Eng. 287, 466 (2002).
[35] Zhiwen Jin, Guo Liu, and Jizheng Wang, AIP Adv. 3, 052113 (2013).
[36] A. Prakash, J. Ouyang, J.-L. Lin, and Y. Yang, J. Appl. Phys. 100, 054309 (2006).
[37] S.-H. Lee, S.-H. Oh, Y. Ji, J. Kim, R. Kang, D. Khim, S. Lee, J.-S. Yeo, N. Lu, M. J. Kim, H. C. Ko, T.-W. Kim, Y.-Y. Noh, and D.-Y. Kim, Org. Electron. 15, 1290 (2014).